Distributed Source Localization with Antenna Arrays and CRB-Based Fusion

Miguel Rivas-Costa and Carlos Mosquera

atlanTTic Research Center, Universidade de Vigo, Vigo, Spain
{mrivascosta,mosquera}@gts.uvigo.es

***Abstract*—Source localization with distributed networks is hindered by the high communication overhead associated with raw data transmission from nodes. We propose a framework for antenna arrays, applicable to both mobile platforms and distributed networks, which compresses the local data in each node into a compact set of Direction-of-Arrivals (DoAs) and power parameters. As the local estimation is highly dependent on the specific hardware architecture, we focus on Hybrid Analog and Digital (HAD) antenna arrays, for which we introduce a two-stage estimator that exploits the structural characterization of the Spatial Covariance Matrix (SCM). Global localization is then performed by a Fusion Center (FC) that must account for the heterogeneous quality of the incoming data. Rather than assuming a specific error distribution, we employ the Cramér-Rao Lower Bound (CRB) as a statistical weighting tool. With this, global estimate accounts for the specific hardware characteristics, link quality and geometry of each node. Simulations indicate that the framework achieves near-efficient localization accuracy.**

***Index Terms*—Direction of arrival, hybrid analog and digital arrays, array signal processing, localization.**

I. INTRODUCTION

Source localization remains a cornerstone of signal processing, with its importance surging alongside the proliferation of distributed networks, such as Unmanned Aerial Vehicle (UAV) swarms and ad-hoc sensor grids [1]–[4]. Historically, sensor networks were primarily composed of passive, single-sensor nodes with limited processing capabilities. However, modern implementations have evolved into active sophisticated systems where nodes are equipped with multi-antenna architectures capable of performing complex local signal processing [5]–[7]. While localization has been extensively developed for single mobile platforms, where a lone agent captures sequential measurements along a trajectory to create virtual network nodes, modern applications are increasingly shifting towards distributed networks of multiple agents. The primary distinction lies in the communication requirement: in distributed networks, data must be transmitted from individual nodes to a central entity, making the available bandwidth a critical and often limiting factor. Regardless of the architecture, the fundamental objective remains to estimate source coordinates from collected signal data. Traditional localization strategies generally bifurcate into two categories:

i) **Bearing-Only Localization (BOL)**. This is a decentralized approach where the individual nodes process their received signals locally to estimate intermediate parameters such as Direction of Arrival (DoA) or Time Difference of Arrival (TDOA). These estimates are then transmitted to a Fusion Center (FC), which fuses them to locate the sources. Historically, BOL techniques have focused on single source scenarios by using the Maximum Likelihood Estimator (MLE) [8], geometric-based approaches [9], techniques based on linearization techniques to reduce complexity [10]–[12] or Machine-Learning techniques [13]. However, in a multi-source environment, BOL requires the FC to solve an additional data association problem [14], correctly pairing intermediate estimates from different nodes to their respective source.

ii) **Direct Position Determination (DPD)**. DPD techniques bypass intermediate parameter estimation. Nodes transmit raw signal data [15]–[20] or sufficient statistics, such as the Spatial Covariance Matrix (SCM), to the FC [21], where sources positions are estimated, typically via multi-dimensional grid searches [22], [23], MUSIC-like algorithms [16], [17], [21], or iterative Expectation-Maximization [20].

Despite the accuracy of DPD, its practical implementation is severely hindered by the high communication demands from every node to the FC, that scales poorly as the number of sensors increases. In addition, a coherent aggregation of the different contributions requires an accurate calibration of the different sensors [24], making BOL the preferred target for this study.

The estimation performance of each sensing unit will be determined by the corresponding multi-antenna architecture. The massive hardware cost associated with Fully Digital (FD) arrays, with a dedicated RF-chain for every antenna, has made Hybrid Analog and Digital (HAD) architectures emerge as a lower cost alternative. However, this cost-saving measure introduces an additional challenge: the signal is compressed at the hardware level before any digital processing can be performed. As a result, local parameter estimation becomes significantly more difficult, an aspect that has received limited attention in the existing literature. For example, [18] considers

This research was funded in part by MICIU/AEI/10.13039/501100011033 FEDER/EU under projects PID2021-122483OA-I00 and PID2022-136512OB-C22. Work supported in part by the Xunta de Galicia (Secretaría Xeral de Universidades) under a Predoctoral Scholarship (cofunded by the European Social Fund) ED481A 2022/407.

DPD-based localization using a HAD architecture; however, the approach is limited to a single source transmitting a sequence that is known *a priori* by all nodes.

In this paper, we address these challenges by proposing a localization framework based on multiple non-coherent arrays [25]. Each node, equipped with a multi-antenna array, employs a two-stage estimator that exploits the structure of the SCM to achieve high-accuracy parameter estimation. This enables the nodes to compress complex spatial observations into a compact set of parameters (DoAs, signal power, and noise power). A FC then performs global fusion using a weighted bearing-only localization method based on the Cramér–Rao Bound (CRB). The CRB serves as a statistical weighting mechanism, ensuring that the contribution of each node is prioritized according to the reliability of its estimates. As a result, the framework enables accurate source localization across unsynchronized sub-arrays while drastically reducing communication requirements.

Notation: We use upper-case boldface letters to represent matrices and vectors, respectively. $\boldsymbol{I}_N$ denotes the $N \times N$ identity matrix. The ℓ_2-norm and expectation are represented by $\|\cdot\|_2$ and $\mathbb{E}[\cdot]$, respectively. The operator $\mathrm{diag}(a_1, \ldots, a_N)$ denotes a diagonal matrix with entries $a_1, \ldots, a_N$ on its main diagonal, while $\mathrm{blkdiag}(\boldsymbol{A}_1, \ldots, \boldsymbol{A}_N)$ refers to a block-diagonal matrix with matrices (or vectors) $\boldsymbol{A}_1 \ldots, \boldsymbol{A}_N$. Finally, $\hat{\boldsymbol{a}}$ denotes an estimate of the vector (or matrix) $\boldsymbol{a}$.

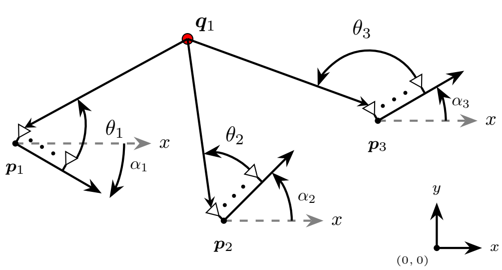

Fig. 1: Geometry for a single-source ($L = 1$) and three nodes ($J = 3$). The diagram illustrates the relationship between the global coordinate system, subarray positions $\boldsymbol{p}_j$, orientation angles α_j, and local DoAs θ_j.

II. Signal model

A. Distributed Network Characterization

We consider a distributed sensing network composed of a Fusion Center (FC) at the origin $(0, 0)$ of a 2-D coordinate system, J sensing nodes and L emitters. The number of emitters is supposed to be known *a priori* in all the nodes and at the FC. Results are also applicable to a moving observer performing estimates at J different locations of a set of fixed sources. Each node $j \in \{1, \ldots, J\}$ is equipped with a Uniform Linear Array (ULA) consisting of N_j antennas and $N_{\mathrm{RF},j}$ RF-chains ($N_{\mathrm{RF},j} \le N_j \ \forall j$). The antenna spacing of each array is fixed at $d_j = \lambda/2 \ \forall j$, where λ is the operating wavelength. As illustrated in Fig. 1, the known global position of the j-th node is defined by its reference antenna element $\boldsymbol{p}_j = [p_{x,j,1}, p_{y,j,1}]^T$, with its orientation relative to the global x-axis represented by the angle $\alpha_j \in [-\pi/2, \pi/2]$. Consequently, the coordinates of the n-th antenna element in the j-th node are mapped as:

$$\boldsymbol{p}_{j,n} = \boldsymbol{p}_j + (n-1)d \begin{bmatrix} \cos(\alpha_j) \\ \sin(\alpha_j) \end{bmatrix} \ n = 1, \ldots, N_j. \quad (1)$$

The L emitters are located at unknown coordinates $\boldsymbol{q}_\ell = [q_{x,\ell}, q_{y,\ell}]^T$ for $\ell = 1, \ldots, L$. Geometrically, the signal from the ℓ-th emitter arrives at the j-th array with a *local* Direction of Arrival (DoA) $\theta_{j,\ell}(\boldsymbol{q}_\ell) \in [0, \pi] \ \forall j, \ell$. This local angle is linked to the global geometry through the relation

$$\theta_{j,\ell}(\boldsymbol{q}_\ell) = \mathrm{arctan2}(q_{y,\ell} - p_{y,j}, q_{x,\ell} - p_{x,j}) - \alpha_j. \quad (2)$$

To simplify the notation, we suppress the explicit dependence on $\boldsymbol{q}_\ell$ and refer to the angle simply as $\theta_{j,\ell}$.

B. Node Received Signal Characterization

We assume that node j applies Hybrid Analog and Digital (HAD) beamforming characterized by a *codebook* of K_j matrices $\{\boldsymbol{B}_j(t) \in \mathbb{C}^{N_j \times N_{\mathrm{RF},j}}\}_{t=1}^{K_j}$. To ensure that the noise power remains invariant after beamforming, we enforce the semi-unitary constraint $\boldsymbol{B}_j^H(t)\boldsymbol{B}_j(t) = \boldsymbol{I}_{N_{\mathrm{RF},j}} \ \forall\, t, j$ [26]. This formulation is sufficiently general to encompass a range of architectures, for example, for $\boldsymbol{B}_j(t) = \boldsymbol{I}_{N_j}$ the node j employs a Fully Digital array. After down-conversion and sampling, the received signal vector $\boldsymbol{y}_j(t) \in \mathbb{C}^{N_{\mathrm{RF},j} \times 1}$ is modeled as

$$\boldsymbol{y}_j(t) = \boldsymbol{B}_j^H(t)(\boldsymbol{A}_j(\boldsymbol{\theta}_j)\boldsymbol{s}_j(t) + \boldsymbol{n}_j(t)) \ \ 1 \le t \le K_j, \quad (3)$$

where $\boldsymbol{A}_j(\boldsymbol{\theta}_j) \triangleq [\boldsymbol{a}_j(\theta_{j,1}), \ldots, \boldsymbol{a}_j(\theta_{j,L})]$ represents the array manifold matrix. This matrix is formed by the steering vectors of the L sources. For ULAs, the steering vector corresponding to the ℓ-th source is defined as:

$$\boldsymbol{a}_j(\theta_{j,\ell}) \triangleq [1, e^{j\pi\cos\theta_{j,\ell}}, \ldots, e^{j(N_j-1)\pi\cos\theta_{j,\ell}}]^T \quad (4)$$

The vector $\boldsymbol{s}_j(t) \in \mathbb{C}^{L \times 1}$ represents the emitted signals as observed in node j, modeled as a zero-mean white random process with diagonal covariance $\boldsymbol{R}_{s,j} \triangleq \mathbb{E}[\boldsymbol{s}_j(t)\boldsymbol{s}_j^H(t)] = \mathrm{diag}(\sigma_{s,j,1}^2, \ldots, \sigma_{s,j,L}^2)$. The noise $\boldsymbol{n}_j(t) \in \mathbb{C}^{N_j \times 1}$ is zero-mean white complex Gaussian noise with covariance matrix $\sigma_{n,j}^2 \boldsymbol{I}_{N_j}$. Due to the lack of temporal synchrony among the different signal captures, we assume non-coherent processing [25], where the noise and emitted signals are statistically independent across different nodes. The spatial information at each node is completely captured by $2L+1$ parameters representing the DoAs and powers. These are collected into the parameter vector $\boldsymbol{\eta}_j \in \mathbb{R}^{(2L+1)\times 1}$ as

$$\boldsymbol{\eta}_j \triangleq [\boldsymbol{\theta}_j^T, (\boldsymbol{\sigma}_{s,j}^2)^T, \sigma_{n,j}^2]^T \quad 1 \le j \le J, \quad (5)$$

where $\boldsymbol{\theta}_j \triangleq [\theta_{j,1}, \ldots, \theta_{j,L}]^T$ and $\boldsymbol{\sigma}_{s,j}^2 \triangleq [\sigma_{s,j,1}^2, \ldots, \sigma_{s,j,L}^2]^T$. These parameters are embedded into the Spatial Covariance Matrix (SCM) $\boldsymbol{R}_j(\boldsymbol{\eta}_j) \in \mathbb{C}^{N_j \times N_j}$ of the underlying Fully Digital (FD) array, which reads as

$$\boldsymbol{R}_j(\boldsymbol{\eta}_j) = \sum\nolimits_{\ell=1}^{L} \sigma_{s,j,\ell}^2 \boldsymbol{a}_j(\theta_{j,\ell})\boldsymbol{a}_j^H(\theta_{j,\ell}) + \sigma_{n,j}^2 \boldsymbol{I}_{N_j}. \quad (6)$$

Note that the SCM $\boldsymbol{R}_j(\boldsymbol{\eta}_j) \triangleq \mathbb{E}[\boldsymbol{x}_j(t)\boldsymbol{x}_j^H(t)]$, with $\boldsymbol{x}_j(t) = \boldsymbol{A}_j(\boldsymbol{\theta}_j)\boldsymbol{s}_j(t) + \boldsymbol{n}_j(t)$, is not directly observable due to the beamforming in (3). This is a Hermitian Toeplitz matrix and, consequently, can be completely defined by $2N_j - 1$ unique entries. We define the *spatial covariance sequence* as the vector that aggregates these set of entries as

$$\boldsymbol{r}_j \triangleq [\boldsymbol{R}_j^*[N_j, 1], \ldots, \boldsymbol{R}_j[1, 1], \ldots, \boldsymbol{R}_j[N_j, 1]]^T. \quad (7)$$

III. Node-level Parameter Estimation

Unlike Direct Position Determination, where nodes transmit an estimate of the SCM $\hat{\boldsymbol{R}}_j$, requiring $\sum_{j=1}^J N_j^2$ real parameters, our framework only transmits the compact set $\{\hat{\boldsymbol{\theta}}_j, \hat{\boldsymbol{\sigma}}_{s,j}, \hat{\sigma}_{n,j}\}$. This reduces the feedback overhead to just $J \cdot (2L+1)$ real parameters, where typically $L \ll N_j$.

We now describe the proposed two-stage algorithm for the estimation of $\{\hat{\boldsymbol{\theta}}_j, \hat{\boldsymbol{\sigma}}^2_{s,j}, \hat{\sigma}^2_{n,j}\}$ at each node $j = 1, \ldots, J$. Unlike FD architectures, for which parameter estimation is well-established [27], HAD systems present a unique challenge due to the inherent signal compression. Methods based on covariance reconstruction are usually preferred for better resolution. In this regard, we apply recent results in [28] to obtain the estimate $\hat{\boldsymbol{r}}_j$ of the spatial covariance sequence (7). This estimate is asymptotically complex Gaussian distributed with mean $\boldsymbol{r}_j = \mathbb{E}[\hat{\boldsymbol{r}}_j]$ and covariance matrix $\boldsymbol{\Sigma}_{\boldsymbol{r}_j} \triangleq \mathbb{E}[(\hat{\boldsymbol{r}}_j - \boldsymbol{r}_j)(\hat{\boldsymbol{r}}_j - \boldsymbol{r}_j)^H]$. In the following, a consistent estimate $\hat{\boldsymbol{\Sigma}}_{\boldsymbol{r}_j}$ of $\boldsymbol{\Sigma}_{\boldsymbol{r}_j}$ will be used due to the unavailability of the true covariance [28].

Each node $j = 1, \ldots, J$ applies a two-stage algorithm. In the first stage, the SCM $\hat{\boldsymbol{R}}_j$ is built from $\hat{\boldsymbol{r}}_j$, and then Root-MUSIC [27] is applied to extract the corresponding estimate $\hat{\boldsymbol{\theta}}_j$. In the second stage, signal and noise powers are obtained. Note that conventional power estimation algorithms rely on the eigenvalues of the SCM; however, because our estimate $\hat{\boldsymbol{R}}_j$ is not guaranteed to be semi-definite positive, standard eigenvalue-based methods are inapplicable. To bypass this limitation, we exploit the linear relationship between the spatial covariance sequence and the powers. Specifically, $\boldsymbol{r}_j$ satisfies

$$\boldsymbol{r}_j = \boldsymbol{\mathcal{A}}_j(\boldsymbol{\theta}_j)\left[(\boldsymbol{\sigma}^2_{s,j})^T \quad \sigma^2_{n,j}\right]^T, \quad (8)$$

where $\boldsymbol{\mathcal{A}}_j(\boldsymbol{\theta}_j) \triangleq [\tilde{\boldsymbol{a}}_j(\theta_{j,1}), \ldots, \tilde{\boldsymbol{a}}_j(\theta_{j,L}), \boldsymbol{e}_{N_j}]$, with $\tilde{\boldsymbol{a}}_j(\theta_{j,\ell}) \triangleq [e^{-j\pi(N_j-1)\cos\theta_{j,\ell}}, \ldots, 1, \ldots, e^{j\pi(N_j-1)\cos\theta_{j,\ell}}]^T$ and $\boldsymbol{e}_{N_j} \triangleq [0, \ldots, 1, \ldots, 0]^T$.

Thus, utilizing the DoA estimates $\hat{\boldsymbol{\theta}}_j$ obtained in the first stage, the signal and noise powers are recovered by solving the weighted covariance matching optimization problem

$$\begin{bmatrix}\hat{\boldsymbol{\sigma}}^2_{s,j}\\ \hat{\sigma}^2_{n,j}\end{bmatrix} = \underset{\{\boldsymbol{\sigma}^2_{s,j}, \sigma^2_{n,j}\}}{\arg\min} \left\| \hat{\boldsymbol{\Sigma}}_{\boldsymbol{r}_j}^{-1/2}\left(\hat{\boldsymbol{r}}_j - \boldsymbol{\mathcal{A}}(\hat{\boldsymbol{\theta}}_j)\begin{bmatrix}\boldsymbol{\sigma}^2_{s,j}\\ \sigma^2_{n,j}\end{bmatrix}\right)\right\|_2^2, \quad (9)$$

for which the closed-form solution reduces to

$$\begin{bmatrix}\hat{\boldsymbol{\sigma}}^2_{s,j}\\ \hat{\sigma}^2_{n,j}\end{bmatrix} = (\boldsymbol{\mathcal{A}}^H(\hat{\boldsymbol{\theta}}_j)\hat{\boldsymbol{\Sigma}}_{\boldsymbol{r}_j}^{-1}\boldsymbol{\mathcal{A}}(\hat{\boldsymbol{\theta}}_j))^{-1}\boldsymbol{\mathcal{A}}(\hat{\boldsymbol{\theta}}_j)^H\hat{\boldsymbol{\Sigma}}_{\boldsymbol{r}_j}^{-1}\hat{\boldsymbol{r}}_j. \quad (10)$$

IV. Joint Localization at the Fusion Center

As discussed in Section I, a prerequisite for BOL in multi-source scenarios is the data association problem, consisting of pairing DoA estimates from different nodes to their respective sources. This step is outside the scope of the present work; we assume it has been performed by some existing technique (e.g., [14]), providing the Fusion Center (FC) has access to the correctly associated DoAs along with their corresponding signal and noise power estimates. . Upon receiving the J sets of local estimates $\{\hat{\boldsymbol{\eta}}_j\}_{j=1}^J$ in (5), the FC fuses this information to estimate the concatenate source position vector $\boldsymbol{q} = [\boldsymbol{q}_1^T, \ldots, \boldsymbol{q}_L^T]^T \in \mathbb{R}^{2L\times 1}$, where $\boldsymbol{q}_\ell = [q_{x,\ell}, q_{y,\ell}]^T$ (see Fig. 1).

The global localization problem is formulated as a Weighted Non-Linear Least Squares (W-NLLS) minimization. Since the exact distribution of the received DoAs $\hat{\boldsymbol{\theta}}_j$ is generally unknown, we leverage the Cramér-Rao Bound (CRB) matrix of the DoAs, denoted as $\boldsymbol{C}_{\theta_j}(\boldsymbol{\eta}_j) \in \mathbb{R}^{L\times L}$ [26], as a statistical proxy to weigh the measurements. Incorporating the CRB allows the FC to account for the heterogeneous nature of the network, including diverse node geometry, varying hardware architectures (e.g., number of antennas or RF-chains), and local signal and noise powers. The weighted W-NLLS cost function is formulated as

$$\hat{\boldsymbol{q}} = \arg\min_{\boldsymbol{q}} \sum_{j=1}^J \|\boldsymbol{C}_{\theta_j}(\hat{\boldsymbol{\eta}}_j)^{-1/2}(\hat{\boldsymbol{\theta}}_j - \boldsymbol{\theta}_j(\boldsymbol{q}))\|_2^2. \quad (11)$$

Since the true CRB depends on the unknown values $\boldsymbol{\eta}_j$, we employ the plug-in estimates $\boldsymbol{C}_{\theta_j}(\hat{\boldsymbol{\eta}}_j)$.

While (11) typically requires a multidimensional non-linear optimization, it can be simplified under the assumption of small estimation errors. Specifically, using the linearization $\hat{\boldsymbol{\theta}}_j - \boldsymbol{\theta}_j(\boldsymbol{q}) \approx \boldsymbol{D}_j^{-1}(\hat{\boldsymbol{B}}_j\boldsymbol{q} - \hat{\boldsymbol{c}}_j)$, as seen in Stansfield-type estimators [10], [11], we approximate (11) as a Weighted Linear Least Squares (W-LLS) problem:

$$\hat{\boldsymbol{q}} = \arg\min_{\boldsymbol{q}} \sum_{j=1}^J \|\boldsymbol{C}_{\theta_j}(\hat{\boldsymbol{\eta}}_j)^{-1/2}\boldsymbol{D}_j^{-1}(\hat{\boldsymbol{B}}_j\boldsymbol{q} - \hat{\boldsymbol{c}}_j))\|_2^2, \quad (12)$$

which admits a closed-form solution:

$$\hat{\boldsymbol{q}} = \left(\sum_{j=1}^J \hat{\boldsymbol{B}}_j^T\hat{\boldsymbol{W}}_j\hat{\boldsymbol{B}}_j\right)^{-1}\left(\sum_{j=1}^J \hat{\boldsymbol{B}}_j^T\hat{\boldsymbol{W}}_j\hat{\boldsymbol{c}}_j\right), \quad (13)$$

with $\hat{\boldsymbol{W}}_j \triangleq (\boldsymbol{D}_j\boldsymbol{C}_{\theta_j}(\hat{\boldsymbol{\eta}}_j)\boldsymbol{D}_j)^{-1}$, $\boldsymbol{D}_j \triangleq \mathrm{diag}(d_{j,1}, \ldots, d_{j,L})$ and

$$\hat{\boldsymbol{B}}_j \triangleq \mathrm{blkdiag}(\hat{\boldsymbol{b}}_{j,1}^T, \ldots, \hat{\boldsymbol{b}}_{j,L}^T), \quad (14)$$

$$\hat{\boldsymbol{b}}_{j,l} \triangleq \left[\sin(\hat{\theta}_{j,\ell} + \alpha_j) \quad -\cos(\hat{\theta}_{j,\ell} + \alpha_j)\right]^T, \quad (15)$$

$$\hat{\boldsymbol{c}}_j \triangleq [\hat{c}_{j,1}, \ldots, \hat{c}_{j,L}]^T, \quad (16)$$

$$\hat{c}_{j,\ell} \triangleq p_{x,j}\sin(\hat{\theta}_{j,\ell} + \alpha_j) - p_{y,j}\cos(\hat{\theta}_{j,\ell} + \alpha_j). \quad (17)$$

Note that the diagonal matrix $\boldsymbol{D}_j$ depends on the unknown node-to-source distances $d_{j,l} \triangleq \|\boldsymbol{p}_j - \boldsymbol{q}_\ell\|_2$, creating a circular dependency. Similar reasoning applies to the true CRB in (11). In this regard, we propose an iterative procedure that updates the matrix $\hat{\boldsymbol{W}}_j^{(k)}$ based on the previous estimate $\hat{\boldsymbol{q}}^{(k-1)}$. This process is detailed in Algorithm 1.

V. Simulations

We validate our proposed algorithms using $\text{MC} = 10^4$ independent Monte Carlo runs. Performance is evaluated via the Root Mean Squared Error: $\text{RMSE} = \sqrt{\frac{1}{\text{MC}} \sum_{i=1}^{\text{MC}} \|\boldsymbol{q} - \hat{\boldsymbol{q}}_i\|_2^2}$, where $\boldsymbol{q}$ and $\hat{\boldsymbol{q}}_i$ denotes the true and estimated position vectors, respectively. We benchmark our estimators against the theoretical Root Cramér-Rao Lower Bound (RCRB) [26], localization RCRB [16] and a genie-aided Stansfield estimator [10] with *a priori* known distances. The latter is equivalent to the first iteration of our method initialized with exact distances via $\boldsymbol{W}_j^{(0)} = \boldsymbol{D}_j^{-2}$. We also compare against the joint Received Signal Strength (RSS) and DoA (RSS+DoA) Least Squares estimator from [29], setting its weighting parameter $\lambda \in [0, 1]$, that balances the confidence between RSS and DoA, to $\lambda = 0.5$, due to the absence of prior knowledge. Furthermore, we also represent the results with the scheme in [30], which makes use of RSS+DoA, and assumes *a priori* knowledge of P_s. Since these baseline methods are limited to a single source, we focus on the $L = 1$ scenario for evaluation.

The RMSE for local parameters $\{\hat{\theta}_{j,1}, \hat{\sigma}^2_{s,j,1}, \hat{\sigma}^2_{n,j}\}$ is computed analogously. Assuming transmit power $P_{s,1}$, the received signals $s_j(t) \in \mathbb{C}^{1\times 1}$ are modeled as independent zero-mean white complex Gaussian, with variance $R_{s,j} = \sigma^2_{s,j,1}$. For simplicity, we adopt the path-loss model $\sigma^2_{s,j,\ell} = P_{s,1}/d^2_{j,1}$, with distance $d_{j,1} = \|\boldsymbol{p}_j - \boldsymbol{q}_1\|_2$. Notably, our method remains agnostic to the specific propagation model.

The parameters for the subarrays are summarized as follows: the antenna counts are $N_j \in \{64, 10, 40, 60, 30\}$, the RF chains are $N_{\text{RF},j} \in \{8, 5, 5, 10, 15\}$, and the corresponding orientations are $\alpha_j \in \{-45°, -30°, 0°, 45°, 90°\}$. The positions of the antennas are displayed in Fig. 2a. In this setup, transmitting the full SCMs would require $\sum_{j=1}^{J} N_j^2 = 10296$ real parameters, whereas our framework requires $J \cdot (2L+1) = 15$ instead.

The performance analysis of the proposed framework begins with the local estimation results for subarray $j = 1$, shown in Fig. 2b. While the DoA estimator $\hat{\theta}_{1,1}$ is highly efficient and converges to the RCRB, the second-stage power estimators $\hat{\sigma}^2_{s,1,1}$ and $\hat{\sigma}^2_{n,1}$ are not statistically efficient; however, our results indicate that the subsequent localization stage is remarkably robust to these small local errors. Moving to the global localization performance in Fig. 2c, our proposed iterative W-LLS method clearly outperforms existing literature alternatives. Methods such as RSS+DoA yield high error floors as they do not exploit the statistical characteristics of the signal and often rely on rigid propagation models that are susceptible to environmental mismatches. Similarly, while the Genie Stansfield incorporates distance-based weighting to prioritize near measurements, it fails to account for the specific hardware and statistical heterogeneity of the network, such as varying antenna counts and RF chain configurations, resulting in a performance gap compared to our proposal, which nearly attains the network-wide RCRB. Finally, it is important to note that although the estimator $\hat{\boldsymbol{q}}_1$ obtained via our proposal is generally biased, we observe that this bias vanishes as the signal power $P_{s,1}$ increases.

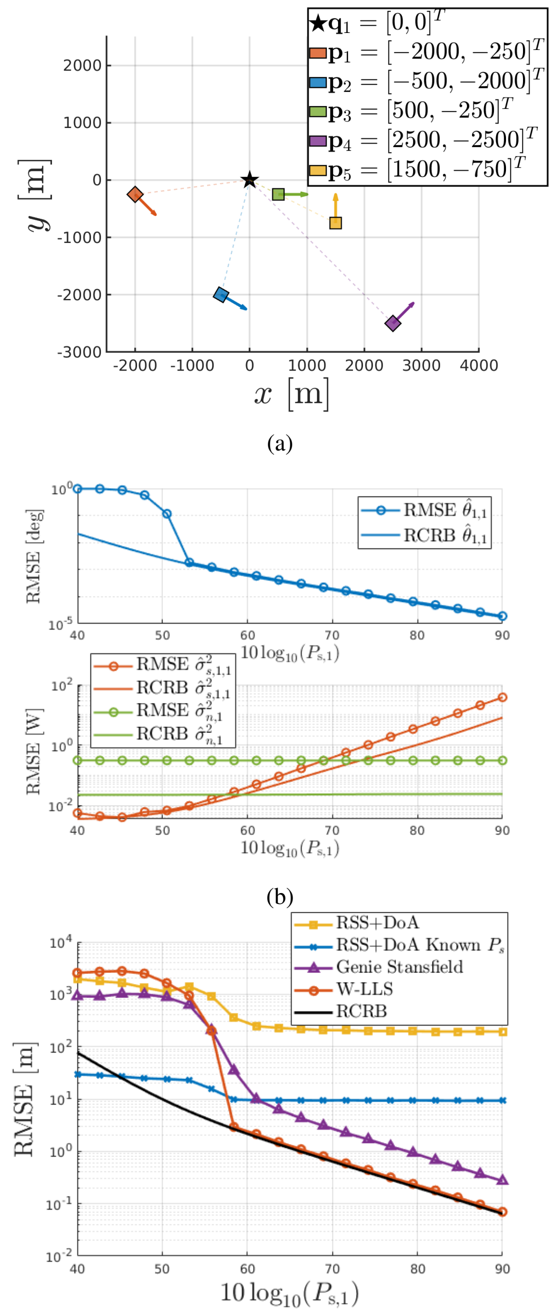

(a)

(b)

(c)

Fig. 2: Performance analysis of the proposed localization framework: (a) Network topology, where squares represent the reference antenna elements $\{\boldsymbol{p}_j\}$ of each subarray and arrows indicate their respective orientations; (b) RMSE and RCRB of local parameter estimation for subarray $j = 1$, including the DOA $\hat{\theta}_{1,1}$, signal power $\hat{\sigma}^2_{s,1,1}$, and noise power $\hat{\sigma}^2_{n,1}$; (c) global source localization RMSE for various estimators compared against the network-wide RCRB.

VI. Conclusion

This paper presents a distributed source localization framework for networks of Hybrid Analog and Digital antenna arrays. At each node, a two-stage estimator exploits the structure of the spatial covariance sequence to efficiently compress local observations into a compact set of DoA and power parameters. At the Fusion Center, these estimates are fused via a CRB-weighted least squares formulation, which naturally accounts for the heterogeneous hardware, geometry, and link quality across nodes. Simulation results demonstrate that the proposed framework achieves near-efficient localization accuracy, closely approaching the theoretical CRB, while substantially reducing the communication overhead.

Algorithm 1 Iterative W-LLS Localization

In: $\hat{\boldsymbol{\eta}}_j^{(0)} = [(\hat{\boldsymbol{\theta}}_j^{(0)})^T, (\hat{\boldsymbol{\sigma}}_{s,j}^2)^T, \hat{\sigma}_{n,j}^2]^T$, $\{\boldsymbol{p}_j, \alpha_j\}$, ϵ, $k_{\max}$.
Out: Refined position $\hat{\boldsymbol{q}}$.

```
Init k = 0 B̂_j, ĉ_j via (14)-(17); Ŵ_j^(0) ← C_θj(η̂_j^(0))^-1; q̂^(0) via (13).
for k = 1 to k_max do
    for j = 1 to J do
        ∀ℓ: θ̂_{j,ℓ}^(k) ← arctan2(q̂_{y,ℓ}^(k-1) − p_{y,j}, q̂_{x,ℓ}^(k-1) − p_{x,j}) − α_j
        ∀ℓ: d̂_{j,ℓ}^(k) ← ‖q̂_ℓ^(k-1) − p_j‖_2

        Update: η̂_j^(k) and D̂_j^(k).
        Ŵ_j^(k) ← (D̂_j^(k) C_θj(η̂_j^(k)) D̂_j^(k))^-1
    end for
    q̂^(k) ← update via (13) using {Ŵ_j^(k)}.
    if ‖q̂^(k) − q̂^(k-1)‖_2 < ϵ then break
    end if
end for
return q̂ = q̂^(k)
```

In LaTeX form:

- **Init** $k=0$ $\hat{\boldsymbol{B}}_j, \hat{\boldsymbol{c}}_j$ via (14)-(17); $\hat{\boldsymbol{W}}_j^{(0)} \leftarrow \boldsymbol{C}_{\theta_j}(\hat{\boldsymbol{\eta}}_j^{(0)})^{-1}$; $\hat{\boldsymbol{q}}^{(0)}$ via (13).
- **for** $k = 1$ **to** $k_{\max}$ **do**
  - **for** $j = 1$ **to** J **do**
    - $\forall \ell$: $\hat{\theta}_{j,\ell}^{(k)} \leftarrow \operatorname{arctan2}(\hat{q}_{y,\ell}^{(k-1)} - p_{y,j}, \hat{q}_{x,\ell}^{(k-1)} - p_{x,j}) - \alpha_j$
    - $\forall \ell$: $\hat{d}_{j,\ell}^{(k)} \leftarrow \|\hat{\boldsymbol{q}}_\ell^{(k-1)} - \boldsymbol{p}_j\|_2$
    - Update: $\hat{\boldsymbol{\eta}}_j^{(k)}$ and $\hat{\boldsymbol{D}}_j^{(k)}$.
    - $\hat{\boldsymbol{W}}_j^{(k)} \leftarrow (\hat{\boldsymbol{D}}_j^{(k)} \boldsymbol{C}_{\theta_j}(\hat{\boldsymbol{\eta}}_j^{(k)}) \hat{\boldsymbol{D}}_j^{(k)})^{-1}$
  - **end for**
  - $\hat{\boldsymbol{q}}^{(k)} \leftarrow$ update via (13) using $\{\hat{\boldsymbol{W}}_j^{(k)}\}$.
  - **if** $\|\hat{\boldsymbol{q}}^{(k)} - \hat{\boldsymbol{q}}^{(k-1)}\|_2 < \epsilon$ **then break**
  - **end if**
- **end for**
- **return** $\hat{\boldsymbol{q}} = \hat{\boldsymbol{q}}^{(k)}$

References

[1] X. Shi, C. Yang, W. Xie, C. Liang, Z. Shi, and J. Chen, "Anti-Drone System with Multiple Surveillance Technologies: Architecture, Implementation, and Challenges," *IEEE Communications Magazine*, vol. 56, no. 4, pp. 68–74, 2018.

[2] L. Xie, S. Song, Y. C. Eldar, and K. B. Letaief, "Collaborative Sensing in Perceptive Mobile Networks: Opportunities and Challenges," *IEEE Wireless Communications*, vol. 30, no. 1, pp. 16–23, 2023.

[3] E. Widdison and D. G. Long, "A Review of Linear Multilateration Techniques and Applications," *IEEE Access*, vol. 12, pp. 26251–26266, 2024.

[4] M. Cobos, F. Antonacci, A. Alexandridis, A. Mouchtaris, and B. Lee, "A survey of sound source localization methods in wireless acoustic sensor networks," *Wireless Communications and Mobile Computing*, vol. 2017, no. 1, p. 3956282, 2017.

[5] G. Wei, B. Zhang, G. Ding, B. Zhao, Y. Wei, and D. Guo, "Massive MIMO-Based Distributed Signal Detection in Multi-Antenna Wireless Sensor Networks," *Sensors*, vol. 20, no. 7, 2020.

[6] Y. Xu, E. G. Larsson, E. A. Jorswieck, X. Li, S. Jin, and T.-H. Chang, "Distributed signal processing for extremely large-scale antenna array systems: State-of-the-art and future directions," *IEEE Journal of Selected Topics in Signal Processing*, vol. 19, no. 2, pp. 304–330, 2025.

[7] A. Ojha and B. Gupta, "Evolving landscape of wireless sensor networks: A survey of trends, timelines, and future perspectives," *Discover Applied Sciences*, vol. 7, p. 825, 2025.

[8] Z. Wang, J.-A. Luo, and X.-P. Zhang, "A Novel Location-Penalized Maximum Likelihood Estimator for Bearing-Only Target Localization," *IEEE Transactions on Signal Processing*, vol. 60, no. 12, pp. 6166–6181, 2012.

[9] Y. Sun, K. C. Ho, L. Gao, J. Zou, Y. Yang, and L. Chen, "Three dimensional source localization using arrival angles from linear arrays: Analytical investigation and optimal solution," *IEEE Transactions on Signal Processing*, vol. 70, pp. 1864–1879, 2022.

[10] K. Doğançay, "Bearings-only target localization using total least squares," *Signal Processing*, vol. 85, no. 9, pp. 1695–1710, 2005.

[11] A. N. Bishop, B. D. O. Anderson, B. Fidan, P. N. Pathirana, and G. Mao, "Bearing-Only Localization using Geometrically Constrained Optimization," *IEEE Transactions on Aerospace and Electronic Systems*, vol. 45, no. 1, pp. 308–320, 2009.

[12] J. Li, L. Wen, Z. Yu, and J. Ding, "State Estimation of Moving Targets Using Sequential Range and Doppler Measurements With Swarm of UAV-Borne Radars," *IEEE Transactions on Aerospace and Electronic Systems*, vol. 61, no. 5, pp. 11904–11918, 2025.

[13] Q. Feng, T. Tang, Y. Zhang, D. Wang, and L. Jiang, "Multistation target localization via direction-of-arrival: An efficient multiagent deep reinforcement learning approach," *IEEE Internet of Things Journal*, vol. 12, no. 19, pp. 40130–40145, 2025.

[14] S. Hu, W. Xue, B. Mu, H. Fang, and Y. Xu, "On Scalable Matching Algorithm for Multi-Targets Over Bearing-Only Sensor Networks," *IEEE Transactions on Signal and Information Processing over Networks*, vol. 11, pp. 724–739, 2025.

[15] J.-A. Luo, Y.-F. Shi, H. Shen-Tu, T. L. Song, D.-L. Peng, and Y. Gu, "Bearing-Only Multi-Target Localization for Wireless Array Networks: A Spatial Sparse Representation Approach," in *2018 21st International Conference on Information Fusion (FUSION)*, pp. 1726–1731, 2018.

[16] B. Demissie, M. Oispuu, and E. Ruthotto, "Localization of multiple sources with a moving array using subspace data fusion," in *2008 11th International Conference on Information Fusion*, pp. 1–7, 2008.

[17] T. Tirer and A. J. Weiss, "High Resolution Direct Position Determination of Radio Frequency Sources," *IEEE Signal Processing Letters*, vol. 23, no. 2, pp. 192–196, 2016.

[18] K. Hao, J. Chen, and Q. Wan, "Direct Position Determination of Indoor Radio Sources Using Hybrid Antenna Arrays," in *2021 IEEE Wireless Communications and Networking Conference (WCNC)*, pp. 1–5, 2021.

[19] X. Fan, L. Liu, and M. Guo, "Direct Position Determination via Joint Sparse Representation of Array Covariance Matrices Based on Angle and Doppler," *IEEE Transactions on Aerospace and Electronic Systems*, vol. 61, no. 6, pp. 17772–17784, 2025.

[20] Z. Wang, B. Tan, M. Valkama, L. Xie, and Q. Wan, "Decentralized Indoor Direct Localization With Multiple Wi-Fi Access Points," *IEEE Transactions on Wireless Communications*, vol. 25, pp. 3091–3105, 2026.

[21] M. Wax and T. Kailath, "A new approach to decentralized array processing," in *ICASSP '84. IEEE International Conference on Acoustics, Speech, and Signal Processing*, vol. 9, pp. 210–213, 1984.

[22] A. Amar and A. Weiss, "Direct position determination of multiple radio signals," in *2004 IEEE International Conference on Acoustics, Speech, and Signal Processing*, vol. 2, pp. ii–81, 2004.

[23] A. Weiss, "Direct position determination of narrowband radio frequency transmitters," *IEEE Signal Processing Letters*, vol. 11, no. 5, pp. 513–516, 2004.

[24] J. Springer, M. Oispuu, and W. Koch, "Joint Calibration and Direct Position Determination for Moving Array Sensors," in *2021 IEEE 24th International Conference on Information Fusion (FUSION)*, pp. 1–8, 2021.

[25] D. W. Rieken and D. R. Fuhrmann, "Generalizing MUSIC and MVDR for multiple noncoherent arrays," *IEEE transactions on signal processing*, vol. 52, no. 9, pp. 2396–2406, 2004.

[26] J. Sheinvald and M. Wax, "Direction finding with fewer receivers via time-varying preprocessing," *IEEE transactions on signal processing*, vol. 47, no. 1, pp. 2–9, 1999.

[27] H. L. V. Trees, *Optimum Array Processing: Detection, Estimation and Modulation Theory, Part IV*. John Wiley & Sons, 2002.

[28] M. Rivas-Costa and C. Mosquera, "Efficient DoA Estimation with Hybrid Linear and Rectangular Arrays Using Compact DFT Codebooks," 2025. arXiv 2509.03488.

[29] S. Wang, B. R. Jackson, and R. Inkol, "Hybrid RSS/AOA emitter location estimation based on least squares and maximum likelihood criteria," in *2012 26th Biennial Symposium on Communications (QBSC)*, pp. 24–29, 2012.

[30] N. Salman, M. W. Khan, and A. H. Kemp, "Enhanced hybrid positioning in wireless networks II: AoA-RSS," in *2014 International Conference on Telecommunications and Multimedia (TEMU)*, pp. 92–97, 2014.